AMERICAN SOCIETY FOR MICROBIOLOGY | Journal of Virology®

VIRUS-CELL INTERACTIONS

Binding of Herpes Simplex Virus 1 UL20 to GODZ (DHHC3) Affects Its Palmitoylation and Is Essential for Infectivity and Proper Targeting and Localization of UL20 and Glycoprotein K

Shaohui Wang,[a] Kevin R. Mott,[a] Kolja Wawrowsky,[a] Konstantin G. Kousoulas,[b] Bernhard Luscher,[c] Homayon Ghiasi[a]

Center for Neurobiology & Vaccine Development, Ophthalmology Research, Department of Surgery, Los Angeles, California, USA[a]; Division of Biotechnology and Molecular Medicine, School of Veterinary Medicine, Louisiana State University, Baton Rouge, Louisiana, USA[b]; Department of Biology, Biochemistry & Molecular Biology, and Psychiatry, Penn State University, University Park, Pennsylvania, USA[c]

ABSTRACT Herpes simplex virus 1 (HSV-1) UL20 plays a crucial role in the envelopment of the cytoplasmic virion and its egress. It is a nonglycosylated envelope protein that is regulated as a γ1 gene. Two-hybrid and pulldown assays demonstrated that UL20, but no other HSV-1 gene-encoded proteins, binds specifically to GODZ (also known as DHHC3), a cellular Golgi apparatus-specific Asp-His-His-Cys (DHHC) zinc finger protein. A catalytically inactive dominant-negative GODZ construct significantly reduced HSV-1 replication *in vitro* and affected the localization of UL20 and glycoprotein K (gK) and their interactions but not glycoprotein C (gC). GODZ is involved in palmitoylation, and we found that UL20 is palmitoylated by GODZ using a GODZ dominant-negative plasmid. Blocking of palmitoylation using 2-bromopalmitate (2-BP) affected the virus titer and the interaction of UL20 and gK but did not affect the levels of these proteins. In conclusion, we have shown that binding of UL20 to GODZ in the Golgi apparatus regulates trafficking of UL20 and its subsequent effects on gK localization and virus replication. We also have demonstrated that GODZ-mediated UL20 palmitoylation is critical for UL20 membrane targeting and thus gK cell surface expression, providing new mechanistic insights into how UL20 palmitoylation regulates HSV-1 infectivity.

IMPORTANCE HSV-1 UL20 is a nonglycosylated essential envelope protein that is highly conserved among herpesviruses. In this study, we show that (i) HSV-1 UL20 binds to GODZ (also known as DHHC3), a Golgi apparatus-specific Asp-His-His-Cys (DHHC) zinc finger protein; (ii) a GODZ dominant-negative mutant and an inhibitor of palmitoylation reduced HSV-1 titers and altered the localization of UL20 and glycoprotein K; and (iii) UL20 is palmitoylated by GODZ, and this UL20 palmitoylation is required for HSV-1 infectivity. Thus, blocking of the interaction of UL20 with GODZ, using a GODZ dominant-negative mutant or possibly GODZ shRNA, should be considered a potential alternative therapy in not only HSV-1 but also other conditions in which GODZ processing is an integral component of pathogenesis.

KEYWORDS virus replication, zinc finger protein, HSV-1, dominant-negative mutant, protein localization, two-hybrid system, virus titer

UL20 is highly conserved among alphaherpesviruses, including herpes simplex virus 1 (HSV-1), pseudorabies virus (PRV), varicella-zoster virus (VZV), bovine herpesvirus 1 (BHV-1), and the gammaherpesvirus Marek's disease virus 2 (MDV-2) (1–5). The HSV-1 UL20 gene encodes a 222-amino-acid (aa) nonglycosylated envelope protein that is

Received 7 June 2017 **Accepted** 13 July 2017

Accepted manuscript posted online 19 July 2017

Citation Wang S, Mott KR, Wawrowsky K, Kousoulas KG, Luscher B, Ghiasi H. 2017. Binding of herpes simplex virus 1 UL20 to GODZ (DHHC3) affects its palmitoylation and is essential for infectivity and proper targeting and localization of UL20 and glycoprotein K. J Virol 91:e00945-17. https://doi.org/10.1128/JVI.00945-17.

Editor Jae U. Jung, University of Southern California

Address correspondence to Homayon Ghiasi, ghiasih@cshs.org.

regulated as a γ1 gene. It plays a crucial role in the envelopment of the cytoplasmic virion and the egress of infectious virus (6, 7). Deletion of UL20 in HSV-1 or PRV results in an up to 100-fold reduction in the production of infectious virus (7–9). In the absence of UL20 protein, virions are trapped in the perinuclear space and in cytoplasmic vesicles of the host cell. It has been shown that UL20 is required for syncytium formation, cytoplasmic envelopment within the *trans*-Golgi network (TGN), and virion transport from the TGN to extracellular spaces during HSV-1 infection (10). The severity of HSV-1 infection in mice is reduced by treatment with ribozymes that target UL20 RNA expression (11).

The Golgi apparatus-specific Asp-His-His-Cys (DHHC) zinc finger protein known as GODZ (also known as DHHC3) has been described as a broad-substrate palmitoyl transferase that is widely expressed in many tissues, including in neurons (12–15). Palmitoyl transferases with this DHHC configuration are present in all eukaryotes and occur as multienzyme families that range in size from 5 to 24 members (16, 17). They play multiple critical roles in physiology and a variety of diseases, including cancer, Huntington's disease, and X-linked intellectual disability (18–22). GODZ is highly conserved between humans, mice, rats, fruit flies, and *Caenorhabditis elegans*, with 97% homology between humans and mice (23). Human GODZ consists of a 327-aa protein, while mouse GODZ is 299 aa long (23). GODZ is broadly expressed in most tissues, including in neurons, and its cellular localization is highly restricted to the *cis* compartment of the Golgi complex (15, 23, 24). Genetic and biochemical studies have established that palmitoylation of proteins on the cytoplasmic face of cell membranes is catalyzed by a family of integral membrane proteins with a conserved Asp-His-His-Cys (DHHC) motif embedded in a cysteine-rich domain (18, 25, 26). GODZ has been shown to palmitoylate various proteins, including transmembrane proteins (23, 27).

In this study, we show that (i) HSV-1 UL20 binds to GODZ, (ii) the UL20-GODZ interaction is required for efficient virus infectivity, (iii) GODZ palmitoylates UL20, and (iv) UL20 palmitoylation by GODZ is required for virus infectivity. Thus, blocking the binding of UL20 to GODZ or blocking the palmitoylation function of UL20 may represent a clinically effective and expedient approach to the reduction of viral replication and the resulting pathology associated with HSV infection.

RESULTS

HSV-1 UL20 binds to GODZ. We found previously that HSV-1 gK binds the signal peptide peptidase (SPP) (28) as well as HSV-1 UL20 (10). We therefore explored the possibility that UL20 also interacts with one or more cellular proteins using a two-hybrid screening assay (BacterioMatch two-hybrid system; Stratagene). UL20 was used as the bait to probe a mouse brain cDNA library. A total of 5×10^6 independent cDNA clones were screened, and selected positive clones were sequenced. NCBI BLAST analysis (29) of collected sequences suggested that HSV-1 UL20 can bind GODZ.

To verify the results of the bacterial two-hybrid screening, we used an immunoprecipitation (IP)-Western pulldown approach. Whole-cell extracts from HeLa cells that transiently expressed a human GODZ-V5 plasmid (Fig. 1A), a UL20-FLAG plasmid (Fig. 1B), or both plasmids were pulled down using protein G beads loaded with either anti-V5, anti-FLAG, or an irrelevant anti-His antibody. The protein bound to the beads was subjected to Western blot analysis. Western blot analysis using anti-V5 antibody or anti-FLAG antibody confirmed that GODZ-V5 was pulled down using the anti-V5 antibody-coupled beads (Fig. 2A), and UL20-FLAG was pulled down using the anti-FLAG antibody-coupled beads (Fig. 2B). Neither GODZ-V5 (Fig. 1A, lane 1) nor UL20-FLAG (Fig. 1B, lane 2) was pulled down from untransfected HeLa cells or from transfected cells by the beads coupled to an irrelevant anti-His antibody (see Fig. S1A in the supplemental material). No protein was pulled down by either the anti-V5 or anti-FLAG antibody-coupled beads from the lysates of untransfected HeLa cells (Fig. 2C, lane 3, and D, lane 3). As shown in Fig. 2C, UL20-FLAG was detected by Western blotting using anti-FLAG antibody of eluates from the anti-V5-coupled beads (lane 4). Conversely, as shown in

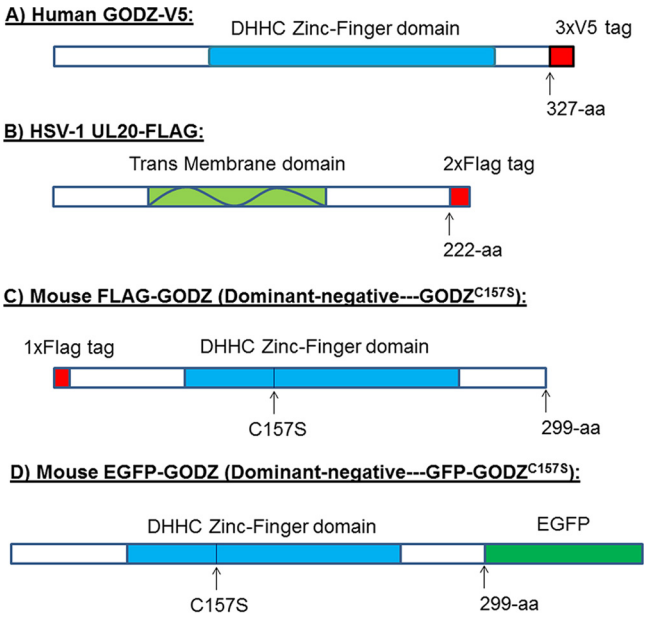

FIG 1 GODZ-V5, UL20-FLAG, and GODZ dominant-negative mutant constructs. (A) The structure of the wild-type human GODZ-V5 molecule of 327 aa is shown with an in-frame insertion of 3 copies of V5 tag on the C terminus. (B) The structure of the HSV-1 UL20 molecule of 222 aa is shown with an in-frame insertion of 2 copies of FLAG tag on the C terminus. (C) The C157S murine GODZ dominant-negative mutant was constructed in which the cysteine (C) at aa 157 was mutated to serine (S). The 299-aa-long murine GODZ dominant-negative mutant is shown with an in-frame insertion of 1 copy of FLAG tag on the amino terminus. (D) Similar to panel C above but with an in-frame insertion of enhanced GFP (EGFP) tag on the carboxy terminus. Genes in panels A and C were inserted into plasmid pcDNA3.1, while genes in panels C and D were inserted into pCMV-Tag 2B.

Fig. 2D, GODZ-V5 was detected by Western blotting using the anti-V5 antibody of the eluates from the anti-FLAG-coupled beads (lane 4).

To test the possibility that GODZ binds to other HSV-1 proteins, we carried out an additional pulldown using HeLa cells infected with HSV-1 strain McKrae and an antibody raised against total anti-HSV-1 that recognizes many HSV-1-encoded proteins but not UL20 and gK. HeLa cells were transfected with GODZ DNA, infected with 1 PFU/cell of HSV-1 strain McKrae, and harvested at 24 h postinfection. The cell lysates were prepared and subjected to immunoprecipitation using anti-GODZ antibody and anti-HSV-1 antibody. The results indicated that although the total anti-HSV-1 antibody immunoprecipitated many of the HSV-1 proteins, it did not pull down GODZ as determined by Western blotting (Fig. S1B). Conversely, anti-GODZ did not pull down any HSV-1-reacting proteins as determined by Western blotting (Fig. S1C). Taken together, these data strongly suggest that UL20 is the only HSV-1-encoded protein that binds to GODZ *in vitro*.

Virus-expressed UL20 colocalizes with cellular GODZ *in vitro*. To determine if UL20 and cellular GODZ colocalize within the HSV-1-infected cells, rabbit skin (RS) cells were infected with VC1 virus expressing FLAG in-frame in the UL20 open reading-frame (30). The cells were stained with anti-GODZ (red) and anti-UL20-FLAG (green) antibodies and analyzed using confocal microscopy. The results verified that GODZ was detectable in the uninfected RS cells and that the anti-FLAG antibody was not reactive (Fig. 3A, Mock-uninfected). In the infected RS cells, colocalization of UL20-FLAG and endogenous GODZ was evident in the merged images (Fig. 3A, Infected). Automated quantitation of the colocalization using Leica software showed that greater than 58% of UL20 was colocalized with endogenous GODZ (Fig. 3B). This colocalization of cellular GODZ and HSV-1-expressed UL20 was consistent with our finding of binding of GODZ and UL20 on pulldown analysis described above (Fig. 2).

GODZ is important for HSV-1 replication *in vitro*. The association of UL20 with endogenous GODZ suggested the possibility that GODZ could influence HSV-1 repli-

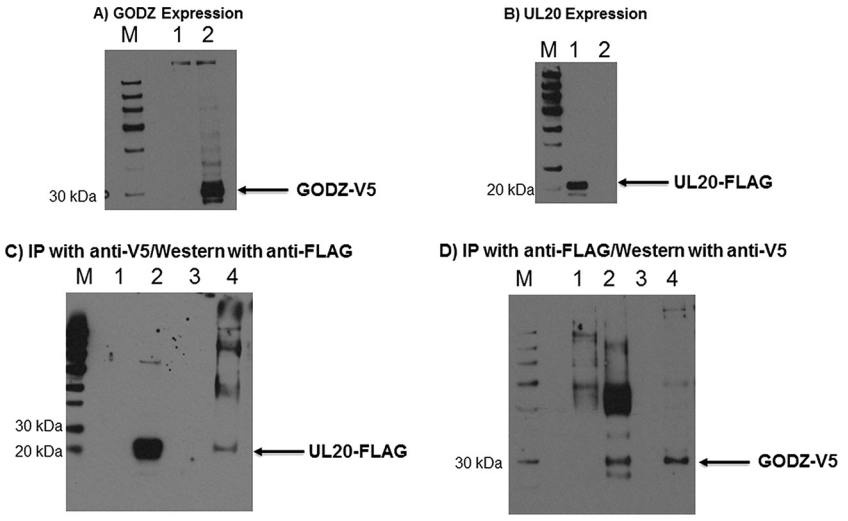

FIG 2 Binding of UL20 to GODZ *in vitro*. HeLa cells were transfected with UL20-FLAG, GODZ-V5, or both plasmids. Lane M, protein size marker. (A) GODZ expression in transfected cells. Cell lysates from GODZ-V5-transfected cells were subjected to Western blot analysis with anti-V5 antibody. Lane 1, untransfected HeLa cells (control); lane 2, GODZ-V5-transfected HeLa cells. (B) UL20 expression in transfected cells. Cell lysates from UL20-FLAG-transfected cells were subjected to Western blot analysis with anti-FLAG antibody. Lane 1, UL20-FLAG; lane 2, untransfected HeLa cells (control). (C) Expression and pulldown of UL20-FLAG. Lysates from cells cotransfected with UL20-FLAG and GODZ-V5 were pulled down with anti-V5 antibody bound to IgG beads, and the bound protein was subjected to Western blot analysis with anti-FLAG antibody. Lane 1, untransfected HeLa cells without immunoprecipitation (IP) (control); lane 2, transfected total cell lysates without IP (control); lane 3, untransfected lysates with IP; lane 4, UL20-FLAG band from transfected lysates with IP. (D) Expression and pulldown of GODZ-V5. Lysates from cells cotransfected with UL20-FLAG and GODZ-V5 were incubated with anti-FLAG antibody bound to IgG beads, and the bound protein was subjected to Western blot analysis with anti-V5 antibody. Lane 1, untransfected HeLa cells without IP (control); lane 2, transfected total cell lysates without IP (control). The intense band is likely to be the cross-linked between UL20 and GODZ. Lane 3, untransfected lysates with IP; lane 4, GODZ-V5 band from transfected lysates with IP.

cation and infectivity. Thus, we used GODZ^{C157S} (the construct shown in Fig. 1C), an inactive mutant of GODZ that, as we showed previously, dimerizes with GODZ and acts as a dominant-negative inhibitor of endogenous GODZ activity (12). RS cells were transfected with a mammalian expression plasmid containing the FLAG-tagged GODZ^{C157S} or with empty vector DNA as a control. The expression of endogenous GODZ and the transfected dominant-negative GODZ was then assessed by Western blotting using anti-GODZ and anti-FLAG antibodies, respectively (data not shown). Thus, to explore whether reduction of GODZ activity affects HSV-1 replication, RS cells were transfected with FLAG-GODZ^{C157S}, followed by infection with 0.1, 0.3, and 0.5 PFU/cell of HSV expressing green fluorescent protein (HSV-GFP$^+$) or HSV-1 strain McKrae. The kinetics of virus replication were quantified by confocal microscopy and fluorescence-activated cell sorter (FACS) analysis using the GFP tag and by determining the amount of infectious virus after infection with various PFU of each virus using a standard plaque assay (Fig. 4). The percentage of HSV-GFP$^+$ cells was significantly lower in cells transfected with GODZ^{C157S} compared with the vector control group at various PFU (Fig. 4A). Similarly, the percentages of HSV-GFP$^+$ cells determined by FACS were lower in cells transfected with FLAG-GODZ^{C157S} than in controls transfected with vector only, independent of the PFU used per cell: at 0.1 PFU/cell, 3% versus 9%, at 0.3 PFU/cell, 6.0% versus 13%, and at 0.5 PFU/cell, 11 versus 23% (Fig. 4B). The mean $\pm$ standard error of the mean (SEM) percentages of HSV-GFP$^+$ cells from three separate FACS analyses are shown in Fig. 4C. There was a significant reduction in the number of HSV-GFP$^+$ cells in the GODZ^{C157S}-transfected compared to vector-transfected cells at all three PFU of GFP-expressing HSV-1 (Fig. 4C). Analysis of the virus titers following infection of cells with GFP-expressing virus (Fig. 4D) indicated that replication of HSV-1 in cells transfected with GODZ^{C157S} was significantly reduced compared to that of controls at the various PFU (Fig. 4D).

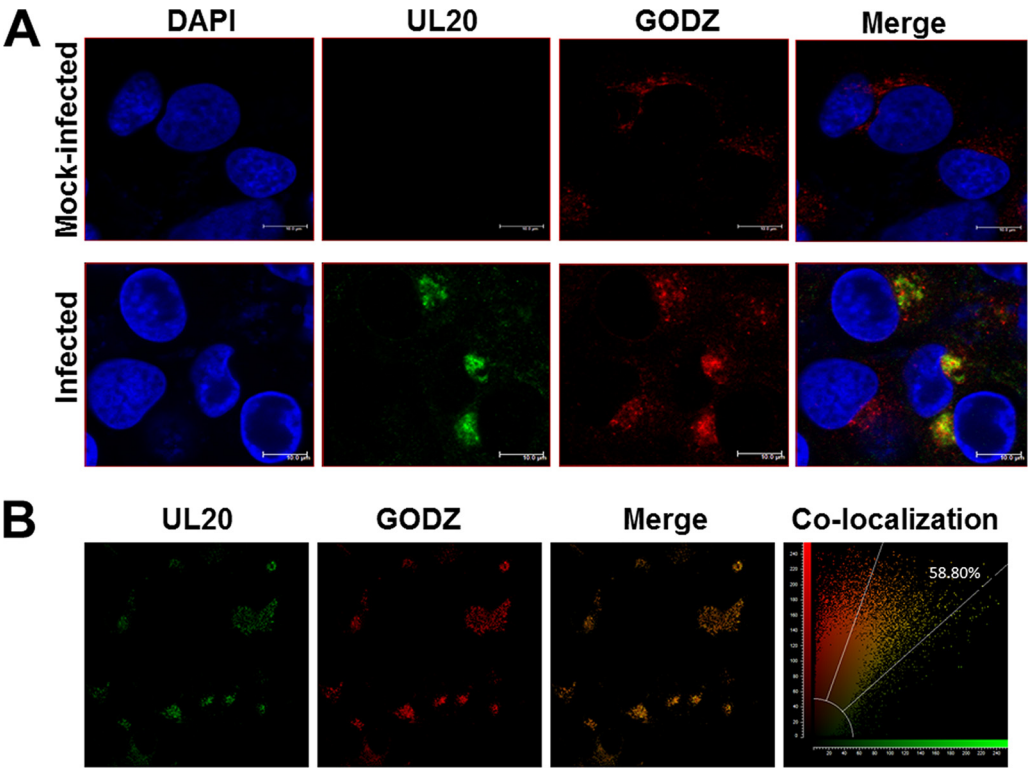

FIG 3 UL20 colocalized with GODZ in HSV-1-infected RS cells. RS cells were infected with 1 PFU/cell of VC1 recombinant HSV-1 expressing FLAG-tagged UL20. Infection was allowed to proceed for 8 h, and then the slides were fixed, blocked, and stained with anti-FLAG (green), anti-GODZ (red), and DAPI nuclear stain (blue). Mock-infected cells were treated similarly and used as a control. Images were acquired using confocal microscopy, and colocalization was visualized as yellow in the merged images. Photomicrographs are shown at a 630× direct magnification. (A) RS cells were mock infected or infected with VC1 virus. (B) Qualitative assessment of colocalization of FLAG-UL20 and GODZ in infected cells as determined using Leica LAS-AF software.

To confirm these results, we used HSV-1 strain McKrae. RS monolayers were transfected and infected as described above, except that HSV-1 strain McKrae was used for infection, and in these experiments, the infected cells were stained with anti-HSV-1 glycoprotein C (gC) antibody. Representative FACS analyses of GODZ^{C157S} and vector control groups at PFU of 0.1, 0.3, and 0.5 are shown (Fig. 4E). At all three PFU, the numbers of HSV-1 gC^{+} cells were lower in the GODZ^{C157S}-transfected cells than in the vector-transfected controls (Fig. 4E). Quantification of the gC^{+} cells from three separate FACS analyses indicated a significant reduction in HSV-1 signal in cells transfected with GODZ^{C157S} compared to the vector control group (Fig. 4F). As was found for the GFP-expressing virus (Fig. 4D), the replication of HSV-1 in cells transfected with GODZ^{C157S} was significantly lower than that of the control group at various PFU when the cells were infected with McKrae virus (Fig. 4G). Collectively, these results confirmed that reducing GODZ activity impairs HSV-1 replication.

The GODZ dominant-negative mutant affects the localization of gK and UL20 but not gC. The above results suggested that the GODZ^{C157S} affected virus replication *in vitro*. Previously, we have shown that UL20 affects cell surface expression of glycoprotein K (gK) (10). We therefore determined whether reducing GODZ activity affected the expression of gK on the cell surface. RS cells were transfected with FLAG-GODZ^{C157S} DNA (Fig. 1C) DNA or vector control DNA as described above, and the transfected cells were infected with VC1 virus for 20 h. To examine cell surface expression of gK, unfixed, unpermeabilized live cells were incubated with anti-V5 antibody (for detection of gK) or with anti-HSV-1-gC antibody as a control. The cell surface expression of gK and gC in vector control and GODZ^{C157S} dominant-negative mutant-transfected cells was examined by indirect immunofluorescence (Fig. 5). Cell surface expression of both gC

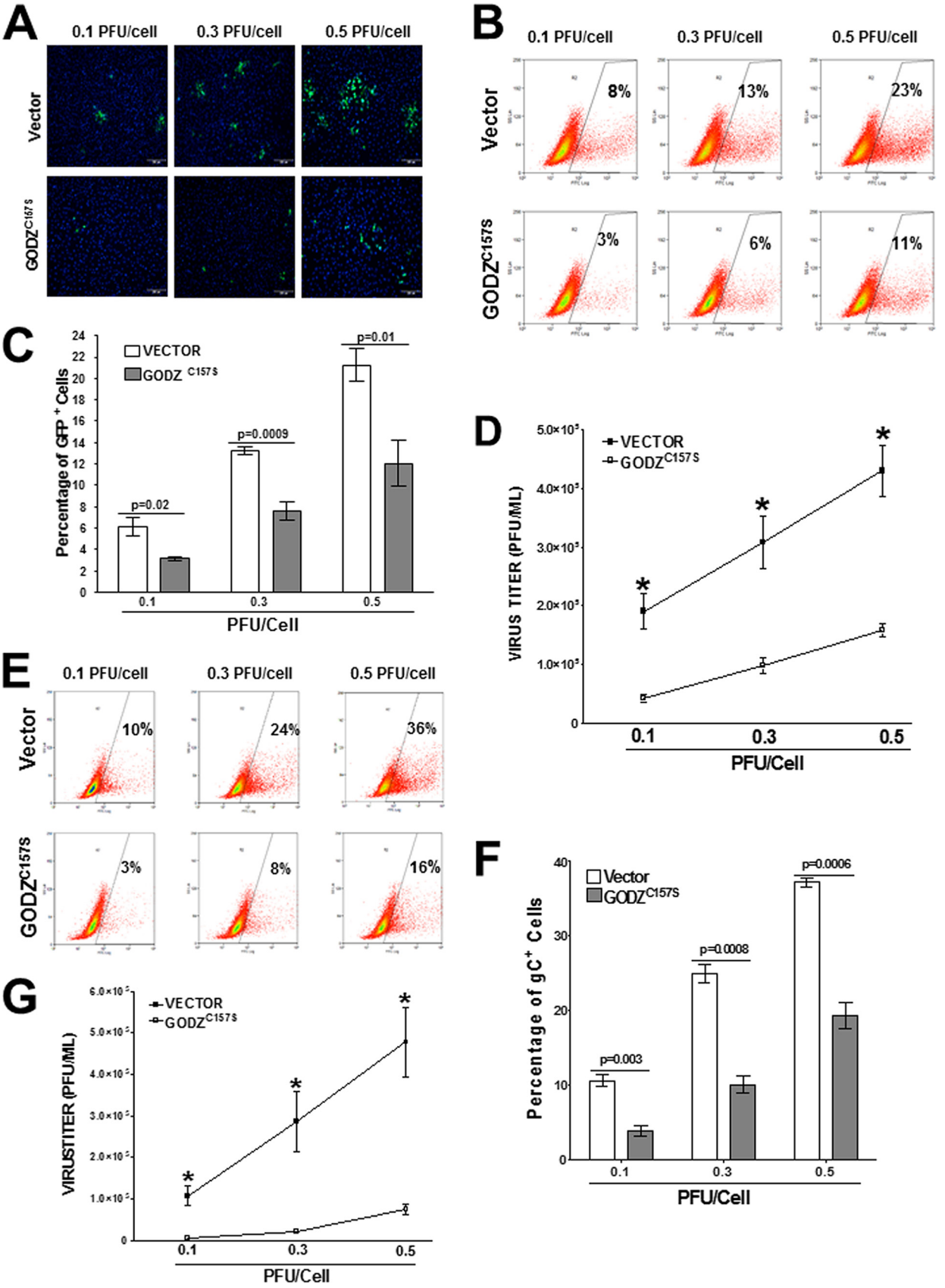

FIG 4 Blocking of HSV-1 replication *in vitro* by the GODZ dominant-negative mutant. (A) Detection of HSV-GFP$^+$ cells by IHC. RS cells were grown to confluence on chamber slides, transfected for 48 h with the GODZ^{S157C} dominant-negative mutant or pCDNA3.1 control vector, and infected with

(Continued on next page)

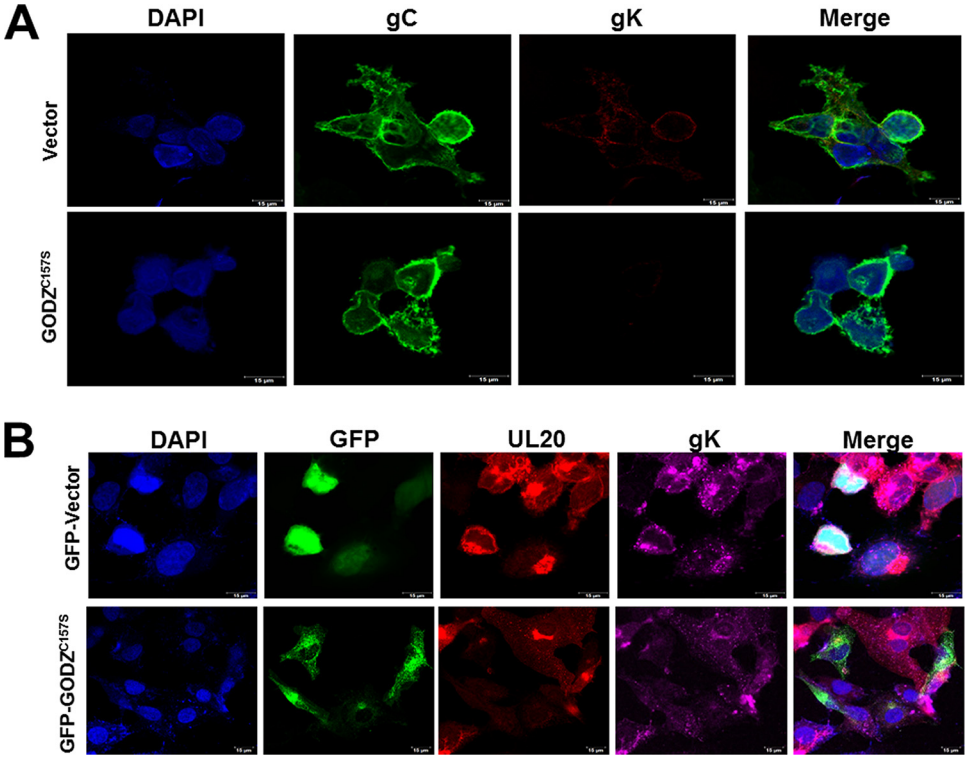

FIG 5 Effect of blockade of the UL20 interaction with GODZ using the GODZ dominant-negative mutant on gK, UL20, and gC transport in HSV-1-infected cells. RS cells were grown to confluence on chamber slides and transfected with GODZ^{C157S}, GFP-GODZ^{C157S}, or their respective control vector DNA for 48 h as in Fig. 3 above, followed by infection with 1 PFU/cell of VC1 virus. (A) At 20 h postinfection, unfixed cells were stained with anti-gC-FITC (green) and anti-V5-Alexa Fluor 647 (red) for detection of gK. DAPI was used for nuclear staining (blue). (B) At 20 h postinfection, slides were fixed, blocked, and stained with anti-FLAG for UL20 and anti-V5 for gK. DAPI was used for nuclear staining (blue) and GFP for transfection efficiency. Photomicrographs are shown at 630× direct magnification.

and gK was readily observed in the infected cells transfected with the vector DNA control (Fig. 5A, Vector), and the merged images further suggested that the gC and gK were expressed on the cell surface in the control vector-transfected infected cells (Fig. 5A, Merge, Vector). As would be anticipated due to the lower gK copy number per cell, expression of gC was significantly higher than that of gK. In contrast, in the cells transfected with the GODZ^{C157S} dominant-negative mutant, although gC was readily detectable on the cell surface (Fig. 5A, GODZ^{C157S}, gC), gK expression was undetectable (Fig. 5A, GODZ^{C157S}, gK). Thus, blocking GODZ function interfered with the cell surface expression of gK but not gC.

Since both UL20 and the GODZ^{C157S} dominant-negative mutant have FLAG as a tag, to determine the effect of the GODZ^{C157S} dominant-negative mutant on localization of UL20 and gK, we transfected RS cells with GFP vector DNA (GFP-Vector) or GFP-

FIG 4 Legend (Continued)
0.1, 0.3, or 0.5 PFU/cell of HSV-GFP$^+$ virus for 20 h. Photomicrographs are shown at 200× direct magnification. (B) Detection of HSV-GFP$^+$ cells by FACS. RS cells were grown on 6-well plates and treated as described above. Cells were trypsinized and fixed, and the presence of GFP$^+$ cells for each PFU was determined by FACS. (C) Quantitation of HSV-GFP$^+$ cells by FACS. Percentages of GFP$^+$ cells treated as in panel B above were quantitated by FACS. Each point represents the mean ± SEM from four independent experiments. (D) Virus titers in transfected cells. RS cells were treated as described above, and virus titers were measured using a standard plaque assay carried out 20 h postinfection. Each point represents the mean ± SEM from three independent experiments. (E) Detection of gC$^+$ cells by FACS. RS cells were grown to confluence on 6-well plates and transfected for 48 h with the GODZ^{S157C} dominant-negative mutant or control vector and infected with 0.1, 0.3, or 0.5 PFU/cell of HSV-1 strain McKrae. At 24 h postinfection, cells were trypsinized, fixed with methanol/acetone, and stained with fluorescein isothiocyanate (FITC)-conjugated HSV-1 gC antibody, and the positive cell populations were analyzed by FACS. (F) Quantitation of gC$^+$ cells by FACS. HSV-1 gC$^+$ cells were treated as in panel E above, and the number of gC$^+$ cells at each PFU was quantitated. Each point represents the mean ± SEM from three independent experiments. (G) Virus titers in McKrae-infected and transfected cells. RS cells were treated as in panel E above, and virus titers were measured by standard plaque assay 24 h postinfection. Each point represents the mean ± SEM from three independent experiments.

GODZ^{C157S} DNA (Fig. 1D) instead of transfection with the FLAG-GODZ^{C157S} dominant-negative mutant (Fig. 1C). Transfected cells were infected with VC1 virus as described above. Infected cells at 20 h postinfection were fixed with methanol/acetone and stained with anti-V5 (for gK) and anti-FLAG (for UL20) antibodies (Fig. 5B). Using this approach, in the vector control-transfected group most of the UL20 expression was found near the cell surface (possibly within the envelope), whereas gK expression was detected both on and near the cell surface (Fig. 5B, GFP-Vector). UL20 and gK GFP were found to be colocalized near the cell surface of the infected cells (Fig. 5B, GFP-Vector, Merge). In contrast, the expression levels and localization of UL20 and gK were affected by transfection with GFP-GODZ^{C157S} DNA (Fig. 5B, GFP-GODZ^{C157S}). Both UL20 and gK were mislocalized primarily within the nucleus, with the effect being more pronounced for gK localization (Fig. 5B, GFP-GODZ^{C157S}). UL20 and gK were not colocalized in the infected cells (Fig. 5B, GFP-GODZ^{C157S}, Merge). Thus, the absence of functional GODZ affected the expression level and localization of UL20 and consequently gK in infected cells.

Palmitoylation is important for HSV-1 replication *in vitro* and proper targeting and localization of UL20 and gK. The above results suggested that GODZ^{C157S} reduced virus replication *in vitro* and affected the localization of UL20 and gK. Given that GODZ is a palmitoyl transferase (12–14, 31) and its binding to UL20 is required for HSV-1 infectivity, we tested whether inhibition of palmitoylation affected HSV-1 replication. There are two broad categories of palmitoylation inhibitors that affect *S*- and *N*-palmitoylation. 2-Bromopalmitate (2-BP) is a lipid-based inhibitor of palmitoylation that has been demonstrated to block palmitoylation of several proteins, including the Src-related tyrosine kinases, Rho family kinases, and H-Ras (32–34). Previously, we have shown that 2-BP blocks GODZ substrate interaction and hence palmitoylation by GODZ (12). Therefore, we used 2-BP to determine if blocking of palmitoylation affects virus replication and gK and UL20 localization without affecting other HSV-1 genes. As 2-BP requires solubilization in dimethyl sulfoxide (DMSO), DMSO-treated cells were therefore used as controls.

We first examined the effect of different concentrations of 2-BP on virus replication in RS cells infected with GFP-expressing HSV-1. Incubation of HSV-1 with 2, 5, 10, 50, or 100 μM 2-BP did not affect virus titer (data not shown), establishing that the inhibitor does not have a direct effect on virus replication. RS cells were treated with the same 2-BP concentrations for 0 to 48 h and then stained with trypan blue. Microscopic examination indicated that the inhibitor was not cytotoxic for the cells (not shown). We then tested the effects of 2-BP on virus replication. RS cells were incubated with 2, 5, 10, 50, or 100 μM 2-BP before and after infection with 0.3 PFU/cell of GFP-expressing HSV-1 (Fig. 6A). FACS analyses indicated that the percentage of GFP$^+$ cells decreased from 32% at 2 μM to only 4% at 100 μM 2-BP, while 65% of DMSO-treated control cells were GFP positive (Fig. 6A). A summary of the effects of various concentrations of 2-BP on GFP expression from three separate experiments is provided in Fig. 6B.

To test the effect of 2-BP on virus titers, we infected RS cells with HSV-1 strain McKrae and treated them as described above. The virus yield was reduced significantly in the presence of 2-BP, in a concentration-dependent manner (Fig. 6C). FACS analyses of RS cells incubated with 50 μM 2-BP before and after infection with 0.1, 0.3, and 0.5 PFU/cell of GFP-expressing HSV-1 indicated that in the presence of 2-BP, the numbers of GFP$^+$ cells were 8% at 0.1 PFU/cell, 16% at 0.3 PFU/cell, and 19% (at 0.5 PFU/cell) (Fig. 6D). In comparison, in the DMSO-treated control group, the percentage of GFP$^+$ cells increased from 36% at the 0.1 PFU/cell to 95% at 0.5 PFU/cell (Fig. 6D). The ability of 2-BP to reduce HSV-1 replication indicates that palmitoylation contributes significantly to HSV-1 replication.

To determine whether treatment of RS cells with 2-BP affected the expression of HSV-1 gK and gC, the cells were incubated with 50 μM 2-BP before and after infection with VC1 virus for 24 h. The cells were then reacted with anti-V5 antibody for detection of gK and with anti-HSV-1-gC antibody. The expression of gK and gC was examined by indirect immunofluorescence staining (Fig. 6E and F). Cell surface expression of both gC

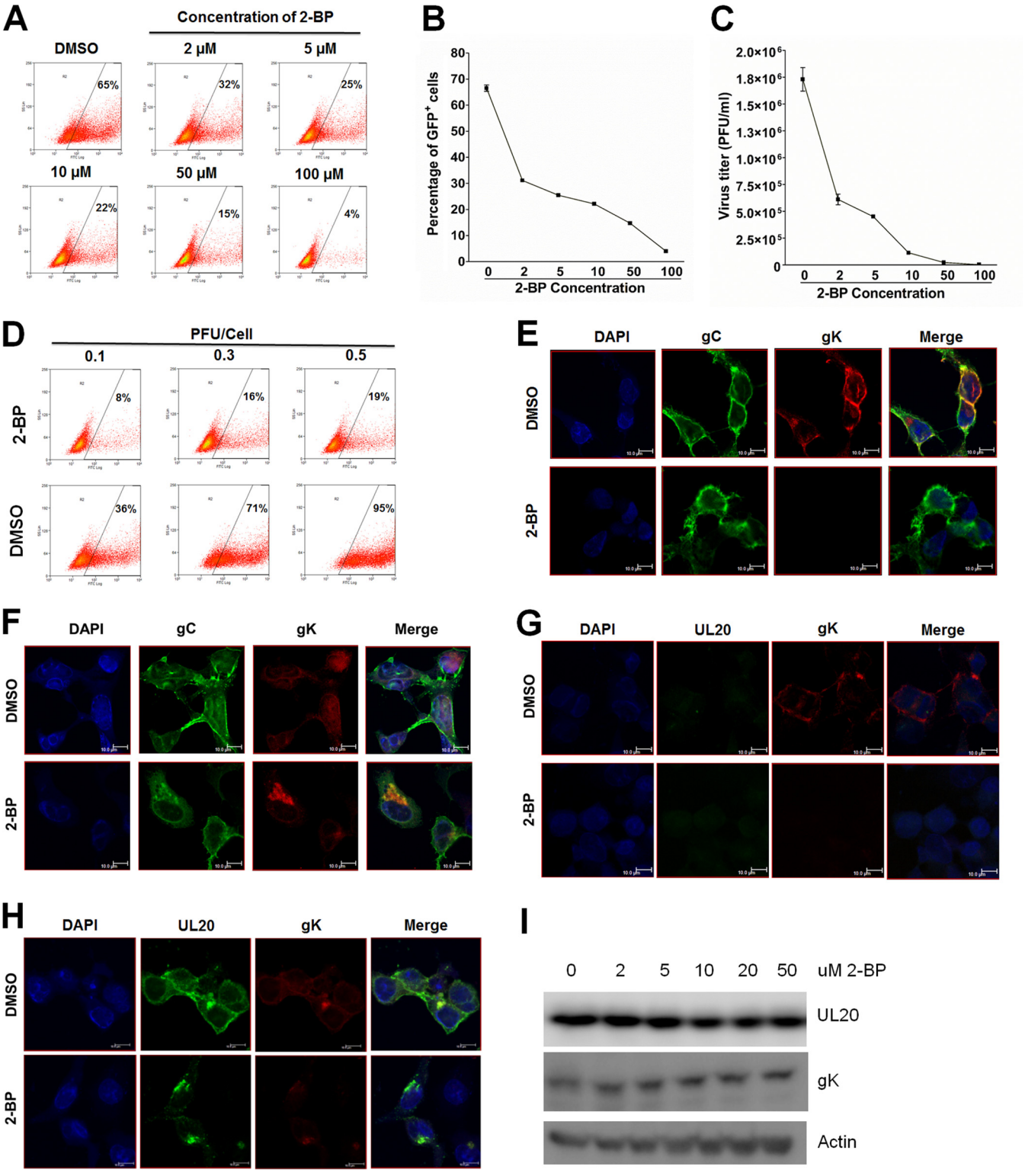

FIG 6 GODZ inhibitor 2-bromopalmitate (2-BP) affects virus replication and alters localization of UL20 and gK in infected cells. (A) Effect of different concentrations of 2-BP on HSV-GFP$^+$ infectivity. RS cells were incubated with 2, 5, 10, 50, and 100 μM 2-BP and infected with HSV-GFP$^+$ virus for 24 h in culture medium containing the corresponding concentration of 2-BP. At 24 h postinfection, cells were fixed and the numbers of GFP$^+$ cells determined by FACS. DMSO-treated RS cells were used as a control. (B) Percentage of GFP$^+$ cells treated with different concentrations of 2-BP. Cells were treated as described above, and the percentage of GFP$^+$ cells from HSV-GFP$^+$-infected cells was quantitated by FACS from three independent experiments. Data are shown as mean ± SEM. (C) Viral titer is reduced by 2-BP. RS cells were treated with different concentrations of 2-BP as described above and infected with HSV-1 strain McKrae. Virus titers were measured using standard plaque assays at 24 h postinfection. Each point represents the mean ± SEM from three independent experiments per 2-BP concentration. (D) Effect of 2-BP on virus replication. RS cells were treated with 50 μM 2-BP as described above and then infected with 0.1, 0.3, and 0.5 PFU/cell of HSV-GFP$^+$ virus. The percentage of GFP$^+$ cells was determined 24 h postinfection by FACS. (E) Cell surface expression of gC and gK in the presence of 2-BP.

(Continued on next page)

and gK was readily observed in the unfixed, control DMSO-treated cells (Fig. 6E, DMSO, Merge), and as anticipated, the expression of gC was higher than the expression of gK. In contrast, cell surface expression of gK was not observed in the unfixed 2-BP-treated cells (Fig. 6E, 2-BP, gK), whereas cell surface expression of gC was readily detectable (Fig. 6E, 2-BP, gC, merge). Similar results were found with fixed cells. In fixed control DMSO-treated cells, both gC and gK were detected at the cell surface and their distribution was similar, as indicated in the merged images (Fig. 6F). On treatment with 2-BP, gC was detected at the surface of the infected cells, whereas gK was not (Fig. 6F, 2-BP), and gK and gC were not colocalized (Fig. 6F, Merge). Thus, blocking of palmitoylation by 2-BP affected the cell surface expression of gK but not gC.

We then determined the localization of UL20 and gK in unfixed and fixed cells, using anti-FLAG antibody for detection of UL20 and anti-V5 antibody to detect gK as described above. In unfixed DMSO-treated infected cells, as expected a cell surface UL20 signal was not detected (Fig. 6G, DMSO, UL20), but gK was detected on the surface of infected cells (Fig. 6G, DMSO, gK, Merge). In the unfixed 2-BP-treated cells, neither a UL20 nor a gK signal was detected (Fig. 6G, 2-BP, gK). In contrast, in fixed DMSO-treated cells both UL20 and gK were readily detectable and similarly distributed near the cell membrane (Fig. 6H, DMSO). In comparison, the membrane UL20 and gK staining and localization were significantly reduced in the fixed 2-BP-treated cells (Fig. 6H, 2-BP). Thus, palmitoylation of UL20 by GODZ regulates UL20 and gK membrane targeting and subcellular localization.

Our results suggested that 2-BP significantly affected virus titers in a dose-dependent manner. To test the possibility that 2-BP modulates the synthesis of UL20 and gK, thereby affecting HSV-1 replication and UL20 and gK localization, we infected RS cells with 1 PFU/cell of VC1 virus for 20 h in the presence of different concentrations of 2-BP (Fig. 6I). Whole-cell lysates were then analyzed by Western blotting using anti-FLAG antibody (for detection of UL20), anti-V5 (for detection of gK), and antiactin as a control. No differences were detected in the levels of UL20, gK, and actin in cells treated with 2, 5, 10, 20, or 50 μM 2-BP versus vehicle-treated control cells (Fig. 6I). Thus, the effects of 2-BP on UL20 and gK cell surface localization reflect a change in protein trafficking and are not due to altered protein expression or stability.

UL20 is palmitoylated. Collectively, the above results suggested that palmitoylation is important for UL20 and gK localization and thus virus replication. We therefore determined the palmitoylation status of UL20 as described in Materials and Methods. In this method, the thioester linkage between palmitate and cysteine is cleaved with neutral hydroxylamine (HAM) and then substituted for with biotin-BMCC to assess the presence of palmitate-modified cysteine by Western blots developed using streptavidin. The omission of HAM provides a rigorous control for false positives (Fig. 7, upper panel). In the absence of HAM and 2-BP and presence of DMSO (−HAM, −2-BP, +DMSO) no palmitoylation was detected (lane 1), while in the presence of HAM and the absence of 2-BP (+HAM, −2-BP, +DMSO) UL20 was palmitoylated (lane 2) (compare lanes 1 and 2 in Fig. 7, upper panel). The palmitoylated protein had a molecular mass of approximately 24 kDa, corresponding to that of UL20 (6). No palmitoylated band was detected when cells were treated with 2-BP, both without HAM (−HAM,

FIG 6 Legend (Continued)

RS cells were grown to confluence on chamber slides, incubated with 50 μM 2-BP or DMSO as described above, and infected with 1 PFU/cell of VC1 virus in the presence of inhibitor for 20 h. Unfixed cells were stained with anti-gC-FITC (green) and anti-V5-Alexa Flour 647 (red) to determine cell surface expression of gK and gC. DAPI was used for nuclear staining (blue). (F) Expression of gC and gK in fixed cells in the presence of 2-BP. RS cells were treated as described above (E), and infected cells were fixed, blocked, and stained with anti-gC-FITC (green) and anti-V5 (red) for gK. DAPI was used for nuclear staining (blue). (G) Localization of UL20 and gK in live cells in the presence of 2-BP. RS cells were grown to confluence on chamber slides, incubated with 50 μM 2-BP as described above, and infected with 1 PFU/cell of VC1 virus in the presence of inhibitor for 20 h. DMSO-treated cells were used as controls. Unfixed cells were stained with anti-FLAG (green) for UL20 and anti-V5-Alexa Flour 647 (red) for gK. DAPI was used for nuclear staining (blue). (H) Localization of UL20 and gK in fixed cells in the presence of 2-BP. RS cells were treated as described above (G), and infected cells were fixed, blocked, and stained with anti-FLAG (green) for UL20 and anti-V5 (red) for gK. DAPI was used for nuclear staining (blue). (I) UL20 and gK protein expression is not affected by 2-BP. RS cells were incubated with different concentrations of 2-BP as in panel A above and infected with 1 PFU/cell of VC1 virus for 24 h. Infected cells were lysed as described in Materials and Methods, equal amounts of protein for each concentration of 2-BP were loaded, and Western blotting was performed using anti-FLAG antibody for detection of UL20, anti-V5 antibody for detection of gK, and antiactin antibody for detection of actin as a control. Photomicrographs are shown at 630× direct magnification.

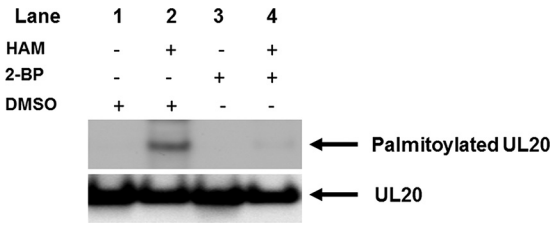

FIG 7 UL20 is palmitoylated. RS cells were incubated with 50 μM 2-BP for 24 h before and after infection. Cells were infected with 1 PFU/cell of VC1 virus for 24 h. DMSO-treated RS cells were used as a control. At 24 h postinfection, cells were harvested and palmitoylation of UL20 was determined as described in Materials and Methods. +, treatment with HAM, 2-BP, or DMSO; –, not treated with HAM, 2-BP, or DMSO. (Upper panel), Lane 1, no palmitoylation band for –HAM, −2-BP, and +DMSO; lane 2, palmitoylated band for +HAM, −2-BP, and +DMSO (compare lane 1 with lane 2); lane 3, no palmitoylation band for –HAM, +2-BP, and −DMSO; lane 4, no palmitoylation band for +HAM, +2-BP, and −DMSO. The blot used to detect palmitoylation in the upper panel was stripped and reprobed with anti-FLAG antibody to detect UL20 as described in Materials and Methods. The lower panel shows detection of UL20 bands with a similar density in all four lanes.

+2-BP, −DMSO, lane 3) and with HAM (+HAM, +2-BP, −DMSO, lane 4) (Fig. 7, upper panel). The presence of UL20 in all lanes was confirmed by stripping of the upper filter of the horseradish peroxidase (HRP)-conjugated streptavidin followed by probing of the membrane with anti-FLAG antibody and HRP-conjugated secondary antibody (Fig. 7, lower panel). The UL20 band was detected in all treatment groups irrespective of the presence or the absence of HAM or 2-BP (Fig. 7, lower panel, lanes 1 to 4). Thus, our results suggest that UL20 is palmitoylated.

GODZ-dependent palmitoylation of UL20. The experiments illustrated above in Fig. 6 using 2-BP show that UL20 is palmitoylated; however, the results do not show that this UL20 palmitoylation is mediated by GODZ. To determine if UL20 palmitoylation is GODZ dependent, we tested whether a GFP-GODZ^{C157S} dominant-negative mutant plasmid could interfere with palmitoylation of UL20. HeLa cells were transfected with UL20 and GFP-GODZ^{C157S} DNA as we describe in Materials and Methods. The control was transfected with UL20 and GFP-Vector. GFP^{+} cells were isolated by FACS, and measurement of palmitoylation was performed as described above (Fig. 6). There was a dramatic reduction in density of the palmitoylated UL20 band in the presence of GFP-GODZ^{C157S} DNA and HAM (Fig. 8, lane 4, +GFP-GODZ^{C157S}, +HAM), while in the presence of HAM and in the absence of GFP-GODZ^{C157S} DNA (−GFP-GODZ^{C157S}, +HAM), UL20 was palmitoylated (Fig. 8, lane 2; compare lane 2 with lane 4 in the upper panel). Quantitation of UL20 palmitoylation revealed that the density of the UL20 protein band in the presence of GFP-GODZ^{C157S} DNA and HAM was reduced

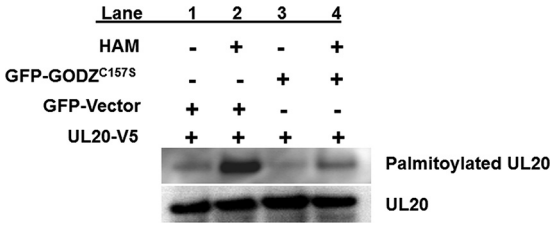

FIG 8 UL20 is palmitoylated by GODZ. HeLa cells were grown to confluence on 6-well plates and transfected with the GFP-GODZ^{S157C} dominant-negative mutant and UL20-V5 DNA or control GFP-Vector and UL20-V5 DNA. At 48 h posttransfection, cells were harvested, GFP^{+} cells were sorted by FACS, and palmitoylation of UL20 was determined as described in Materials and Methods. Lanes (upper panel): 1, +GFP-Vector and −HAM treatment; 2, +GFP-Vector and +HAM treatment; 3, +GFP-GODZ^{C157S} and −HAM treatment; 4, +GFP-GODZ^{C157S} and +HAM treatment. The density of each band was measured using AlphaView SA software (ProteinSimple, San Jose, CA). The density readings are as follows: lane 1, 1,916; lane 2, 6,809; lane 3, 1,351; lane 4, 1,599. Without the subtraction of lane 1 from lane 2 and lane 3 from lane 4, the density of lane 4 compared with lane 2 declined by 77%, while after subtraction of the vector background, it declined by 95%. The lower panel shows detection of UL20 bands with a similar density in all four lanes.

by more than 77% compared with the density of the UL20 protein band in the absence of GFP-GODZ^{C157S} DNA and in the presence of HAM. In control groups, a faint band was detected in the absence of GFP-GODZ^{C157S} DNA and the absence of HAM (Fig. 8, lane 1, −GFP-GODZ^{C157S}, −HAM) and in the presence of GFP-Vector and the absence of HAM (Fig. 8, lane 1, +GFP-Vector, −HAM). However, when the density of the faint band in lane was subtracted from lane 2 and lane 3 was subtracted from lane 4, palmitoylation of band 4 compared with band 2 was reduced by 95%. The presence of UL-20 in all lanes was confirmed by Western blotting with anti-V5 antibody and HRP-conjugated secondary antibody (Fig. 8, lower panel). The UL20 band was detected in all treatment groups irrespective of the presence or the absence of vector or GFP-GODZ^{C157S} (Fig. 8, lower panel, lanes 1 to 4). These results suggest that blocking the function of GODZ by the dominant-negative mutant significantly reduced palmitoylation of UL20.

DISCUSSION

Using a two-hybrid system, we have shown that GODZ specifically binds to UL20, and using a GODZ dominant-negative construct we have demonstrated that GODZ is indeed important for viral replication. UL20 has been shown to interact with HSV-1 gK (35). However, our pulldown experiments using the UL20-expressing plasmid rules out the possibility that the UL20-GODZ interaction is strictly dependent upon complexing with gK or other viral proteins. Moreover, our pulldown of HSV-1-infected RS cells using total HSV-1 antibody, which does not recognize UL20 or gK, failed to precipitate GODZ, and conversely, anti-GODZ failed to precipitate viral proteins.

HSV-1 carries at least 85 genes (6), which are divided into two groups based on whether or not they are essential for virus replication *in vitro*. Both of the genes encoding gK and UL20 are classified as essential for HSV-1 infectivity (7, 8, 35, 36). The membrane-associated UL20 viral protein forms a complex with the gK expressed on virions, and this binding is essential for transport of gK to the cell surface of infected cells (8, 35). Viruses lacking either gK or UL20 are unable to replicate and infect cells efficiently and do not establish latency in neurons (7, 8, 36–40). Previously we reported at least a 3-log reduction in virus infectivity in mutant viruses lacking UL20 or gK (7, 8, 36–40). In the present study; however, we noted that the GODZ dominant-negative mutant reduced virus infectivity by at least 3-fold. These differences between mutant viruses and this study are most likely related to the incomplete blocking of GODZ function by dominant-negative plasmid DNA. In the present study, we have shown that blocking of the UL20 interaction with GODZ also affects gK localization and consequently virus infectivity. However, we cannot rule out the effects of gK function in infectivity in the absence of UL20 binding to GODZ, since we have shown previously that the absence of UL20 binding to gK also affected virus infectivity. Use of an adenovirus vector expressing a hammerhead ribozyme targeting UL20 RNA showed that UL20 expression was reduced significantly and that this was associated with an inhibition of HSV-1 viral replication *in vitro* and *in vivo* (11). Our current results suggest that the effects of the ribozyme reduction in UL20 expression could be associated with a reduction in the binding of UL20 to HSV-1 gK. Previously, we have shown that HSV-1 gK binds to SPP and that short hairpin RNA (shRNA) against SPP, SPP dominant-negative mutants, and SPP inhibitors were all able to reduce HSV-1 titers *in vitro* (28, 41). SPP is an endoplasmic reticulum (ER) protein (42, 43), whereas GODZ is a Golgi protein (23, 44). Previously we reported that gK will not go to the Golgi apparatus without UL20 (10). Thus, collectively our studies suggest a model by which the gK signal in the ER is cleaved by SPP and that UL20 binds to GODZ in the Golgi apparatus and is palmitoylated by GODZ. The cleaved gK is transported to the Golgi apparatus, binds to the palmitoylated UL20, and is then transported in a complex with UL20 to the cell surface of infected cell. This model would predict that interruption of any one of these four interactions SPP-gK-UL20-GODZ could affect virus replication.

Palmitoylation of proteins is a posttranslational modification that occurs through the addition of palmitate to a cysteine residue by *S*-palmitoylation or *N*-palmitoylation (25, 45). Palmitoylation of proteins has been implicated in multiple diseases (46). In the

present study, we have demonstrated that GODZ can bind to HSV-1 UL20. Knockdown of GODZ by dominant-negative GODZ or shRNA suggested that GODZ plays a critical role in normal postsynaptic trafficking of γ2 subunit-containing γ-aminobutyric acid class A receptors ($GABA_A$Rs) and normal GABAergic inhibitory transmission (12, 24). It also has been shown that GODZ-mediated palmitoylation of $GABA_A$Rs is required for the normal assembly and function of GABAergic inhibitory synapses (12, 15, 24). However, the potential for GODZ to modify any of the more than 85 gene products of HSV-1 by palmitoylation or its effects on viral infection had not been explored prior to the present study. We found that blocking of *S*-palmitoylation affected viral replication and altered the localization of UL20 and gK, but not gC. As we have shown here and reported previously, *S*-palmitoylation is regulated by the DHHC family of proteins (16). The mammalian genome contains of at least 24 members of the *DHHC* gene family identified by the presence of the signature DHHC cysteine-rich domain. Based on our binding assay, only GODZ and no other member of the *DHHC* family is involved in UL20 binding. The results of the present study are consistent with the ability of palmitoylation to affect the localization and activity of signaling proteins (47). Previously, it was reported that HSV-1 UL51 is palmitoylated in the Golgi apparatus, but no specific zinc finger protein that could mediate the UL51 palmitoylation was identified, and the effect of this palmitoylation on virus infectivity was not determined (48). HSV-1 UL11 also is palmitoylated, but palmitoylation was not required for its function (49). As we did not see GODZ binding to HSV-1 genes other than UL20 in our pulldown experiments, the UL11 and UL51 palmitoylation may have been mediated by other members of the DHHC family.

Thus, in this study we have shown that UL20, in addition to its role in virion envelopment and egress, is involved in binding the Golgi apparatus-specific protein GODZ. Our results also indicate that UL20 is palmitoylated and that this palmitoylation is dependent on its binding to GODZ. Collectively, the results suggest that UL20 palmitoylation plays an important role in viral replication and possibly virus pathogenesis through mechanisms associated with its palmitoylation by GODZ. Notably, no other protein could compensate for the loss of UL20 in terms of its binding to GODZ. As UL20 is highly conserved among alphaherpesviruses (1, 2, 4), the UL20-GODZ interaction may be of importance to the replication and infectivity of other alphaherpesviruses.

UL20 binding to gK is essential for HSV-1 virus replication and infectivity (8, 35), and gK is involved in exacerbation of HSV-1-associated eye disease and facial dermatitis (50–53). Thus, the UL20-GODZ interaction may be considered a specific therapeutic target for the prevention of corneal infection in patients at risk and in the reduction of the severity of the corneal scarring in patients who have established infections, thereby providing an effective treatment for those individuals suffering from the devastating pathology of HSV-1-induced eye disease.

MATERIALS AND METHODS

Cells and viruses. HeLa cells were obtained from the American Type Culture Collection (ATCC) and grown in Dulbecco's modified Eagle's medium (DMEM) plus 10% fetal bovine serum (FBS). RS (rabbit skin) cells were obtained from Steven L Wechsler (54) and grown in MEM plus 5% FBS as described previously. Triple-plaque-purified HSV-1 strain McKrae was grown in RS cell monolayers as described previously (55, 56). The VC1 virus with V5-tagged gK and the FLAG-tagged UL20 recombinant virus with the HSV-1 F background were grown as we described previously (30). HSV-GFP^+ (a gift from Peter O'Hare, Marie Curie Research Institute, Surrey, United Kingdom) is a recombinant virus that contains the gene encoding a major tegument protein, VP22, linked to green fluorescent protein (GFP) (57, 58) with the HSV-1 strain 17 background and was grown in RS cells.

Two-hybrid system. We used the BacterioMatch two-hybrid system (Stratagene, La Jolla, CA) according to the manufacturer's protocol together with a mouse brain plasmid cDNA library (Stratagene). In this study, we used bait plasmid pBT expressing a λ repressor (λcI)-fused UL20 protein and target plasmid pTRG expressing the α-subunit of RNA polymerase fused to cDNA library-encoded proteins. The *Escherichia coli* reporter strain contained two reporter genes coding for LacZ and carbenicillin resistance ($Carb^r$), under the control of the λcI/α-subunit of RNA polymerase. Additionally, the pBT plasmid contained a chloramphenicol resistance gene (Cam^r), the pTRG plasmid contained a tetracycline resistance gene (Tet^r), and the *E. coli* reporter strain contained a kanamycin resistance gene (Kan^r). To construct pBT-UL20, a cDNA encoding UL20 was amplified by PCR with specific primers containing the BamHI site and inserted into the corresponding sites in the pBT bait plasmid. The mouse brain cDNA

library was amplified and harvested, and final plasmid DNA (pTRG-cDNA mouse brain library) purification was carried out according to the manufacturer's protocol. The *E. coli* reporter strain was transformed with pBT-UL20, and the cDNA library was cloned into pTRG. The transformants were selected on LB agar plates supplemented with Carb, Cam, Tet, and Kan. Putative positive colonies were further tested for LacZ activity by replica plating onto X-Gal (5-bromo-4-chloro-3-indolyl-β-D-galactopyranoside) indicator plates (LB agar supplemented with Cam, Tet, Kan, X-Gal, and β-galactosidase inhibitor) followed by screening for the blue color indicative of LacZ expression. The mouse brain library plasmids were recovered from the positive colonies, and the inserted target cDNA was sequenced using pTRG plasmid-specific primers as described in the manufacturer's protocols. The collected sequences were subjected to NCBI BLAST analysis (29), and the BLAST results showed strong consensus with GODZ sequences as reported previously (23).

Construction and expression of UL20-FLAG and GODZ-V5. The design of the GODZ and UL20 constructs used in this study is shown in Fig. 1. Figure 1A is a schematic diagram of the GODZ construct, which is full-length human GODZ with an in-frame V5 tag at the C terminus. Figure 1B is a schematic diagram of the UL20 construct, which is full-length UL20 with an in-frame FLAG tag at the C terminus. These constructs were synthesized (GenScript, Piscataway, NJ) and inserted into the BamHI site of pcDNA3.1, and the sequences were verified by standard dideoxy sequencing by the UCLA Genotyping and Sequencing Core. The Amaxa Nucleofactor kit (Lonza, Allendale, NJ) was used to transfect HeLa cells (10^6) with a plasmid DNA cocktail containing both UL20-FLAG and GODZ-V5 at a ratio of 1:1 in accordance with the manufacturer's instructions. Protein expression was monitored over 5 days using Coomassie blue protein staining and Western blotting using the Total Western HRP kit (GenScript). The antibodies used were anti-FLAG antibody (DYKDDDDK tag antibody, monoclonal antibody [MAb], mouse, catalog no. A00187; Genscript, Piscataway, NJ) and anti-V5 antibody (GKPIPNPLLGLDST tag antibody, catalog no. A01724) from rabbit (Novus Biologicals, Littleton, CO) or goat (catalog no. A190-119A; Bethyl Lab, Montgomery, TX) diluted according to the manufacturer's instructions. These analyses established that optimal UL20-FLAG and GODZ-V5 expression and recovery occurred at 48 to 72 h posttransfection.

Coimmunoprecipitation. For the coimmunoprecipitation experiments, HeLa cells were cotransfected with the plasmids pcDNA3.1-UL20-FLAG and pcDNA3.1-GODZ-V5 as described above. Cells were harvested at 48 h posttransfection and lysed in the lysis buffer provided with the Classic IP kit (Pierce, Rockford, IL). Prior to use, the lysates were precleared by incubation with control agarose resin for 2 h at 4°C. Coimmunoprecipitations were performed at 4°C unless otherwise indicated using the Pierce Cross-link-IP kit (catalog no. 26147; Thermo Scientific, Rockford, IL). We used the standard cross-linking approach for the preparation of the beads, with the addition of the two homo-bifunctional lysine-specific cross-linkers, disuccinimidyl suberate (DSS) and dithiobis (succinimidylpropionate) (DSP). DSS which is noncleavable, was used to immobilize the capture antibody on the protein A/G agarose resin. DSP, which is cleavable, was used subsequently to produce stable complexes with the captured antigen and its potential binding partners. Approximately 20 μl of protein A/G slurry was washed twice with phosphate-buffered saline (PBS) buffer and incubated with 15 μg of the capture antibody (anti-FLAG antibody [Genscript] or anti-GODZ antibody [Chemicon International, Houston, TX; catalog no. AB9556]) for 1 h at 25°C on an end-over-end mixer. The supernatant was then discarded, and the agarose beads were washed three times with PBS. The agarose beads were then mixed with 50 μl of 2.5 mM DSS solution with end-over-end mixing for 1 h at 25°C. The supernatant was removed, and the agarose was washed three times with 100 μl of 100 mM glycine (pH 2.8). Approximately 1 mg of the precleared cell lysates was mixed with the antibody-cross-linked beads and incubated overnight at 4°C. The following day, 20 μl of 50 mM DSP dissolved in DMSO was added, and the incubation continued for an additional 2 h. The DSP-cross-linking reaction was then quenched by addition of 30 μl of 1 mM Tris-HCl (pH 7.4) and subsequent incubation for 30 min. After removal of the supernatant, the agarose beads were washed 5 times with 600 μl of wash buffer (25 mM Tris, 150 mM NaCl, 5% glycerol, 1 mM EDTA, 1% NP-40). The bound protein was eluted from the washed beads by addition of 50 μl of 2$\times$ Laemmli buffer containing 50 mM dithiothreitol (DTT) and 5% β-mercaptoethanol at 100°C for 10 min.

Western blot analysis. Samples eluted from the anti-FLAG or anti-GODZ cross-linked beads (approximately 25 μl recovered) were loaded directly onto a 4 to 12% Bis-Tris polyacrylamide gel, and electrophoresis was carried out at a constant voltage of 200 V for approximately 30 min. The proteins were then transferred electrophoretically onto nitrocellulose membranes at 35 V for 1 h. The membranes were blocked overnight at 4°C in blocking buffer containing 5% milk and 1% Tween 20 and probed using the One-Hour Western blot kit (GenScript) according to the manufacturer's protocol. Briefly, the membranes were incubated for 5 min in pretreatment solution and then incubated with 1 μg primary antibody (previously incubated in kit-supplied solution Wb-1 containing secondary anti-HRP antibody) for 1 h with anti-GODZ antibody for sample eluted from the anti-FLAG antibody or with anti-FLAG antibody for sample eluted from the anti-GODZ antibody. After being washed 3 times with wash buffer, the membranes were developed using the chemiluminescent HRP substrate and imaged using Kodak Blue Script film. Throughout the study, similar antibody was used for pull down, Western blotting, FACS, and immunohistochemistry (IHC).

Detection of GODZ-UL20 colocalization by confocal microscopy. RS cells were grown to near confluence on Lab-Tek chamber slides and infected with VC1 virus (1 PFU/cell, 8 h). Cells were fixed and incubated with anti-GODZ (Chemicon International) and anti-FLAG (GenScript) to detect UL20. Washed slides were air dried and mounted with 4′,6-diamidino-2-phenylindole (DAPI) Prolong Gold (Invitrogen). The fluorophores were imaged in separate channels by confocal microscopy using a Leica SP5-X confocal microscope with an image acquisition and data analysis system (Leica Microsystems).

Immunostaining. RS cells were transfected with GODZ^{C157S} plasmid or treated with 2-BP as described above, followed by infection with HSV-1 VC1 virus for 20 h. The transfection efficiency of GODZ^{C157S} plasmid DNA was approximately 80%. For live cell staining, anti-V5 (for gK), anti-FLAG (for UL20), or anti-gC (catalog no. 20-251-401549; Genway, San Diego, CA) primary antibodies were added directly to the infected cells, and the cells were incubated for 30 min at 37°C. The cells were then washed three times in PBS, fixed using 4% paraformaldehyde, and incubated with the corresponding secondary antibodies. For fixed cell staining, cells were washed with cold PBS and then fixed using 1:1 methanol-acetone at −20°C for 20 min. Fixed cells were blocked using Sea Block blocking buffer (Thermo Fisher Scientific) for 1 h at room temperature, incubated with the indicated primary antibodies for 2 h, washed 4 times with PBS, and then incubated with the corresponding secondary antibodies for 2 h at room temperature. Slides were washed with PBS, mounted with Prolong Gold (Invitrogen), and analyzed using the Leica SP5-X confocal microscopy system (Leica Microsystems).

FACS. For fluorescence-activated cell sorting (FACS), cells were harvested by centrifugation, resuspended in 4% paraformaldehyde, or sorted without fixing with paraformaldehyde using a multicolor five-laser LSR II instrument or FACSAria II cell sorter (BD Bioscience, San Diego, CA).

Construction and expression of the GODZ dominant-negative mutant. The construction of the N-terminally FLAG-tagged GODZ dominant-negative mutant GODZ^{C157S} was previously described (12, 15) (Fig. 1C). RS cells were grown to near confluence in 6-well plates or Lab-Tek chamber slides and transfected with the GODZ^{C157S} plasmid using JetPrime (Polyplus, Waltham, MA). Transfection was allowed to proceed for 48 h. The cells were then infected with 0.1, 0.3, or 0.5 PFU/cell of HSV-1 strain McKrae, HSV-GFP$^+$ virus, or VC1 virus. After the indicated periods of time, the HSV-1 titer was measured using a standard plaque assay on RS cells as we described previously (54). The number of live GFP$^+$ cells was monitored by confocal imaging and FACS analysis, while expression of gK, UL20, and gC was monitored by IHC.

Analysis of effect of 2-BP on colocalization and virus titers. RS cells were grown to confluence and incubated with 2, 5, 10, 20, 50, or 100 μM 2-BP and then infected with HSV-GFP$^+$ virus, as described above, for 24 h. Virus titers in infected cells were determined using a standard plaque assay, and the numbers of GFP$^+$ cells were determined by FACS analysis. Based on cell viability following incubation with the different concentrations of 2-BP, we chose to use 50 μM 2-BP for our subsequent experiments. As described above, in the presence of 50 μM 2-BP, cells were infected for 24 h with 0.1, 0.3, or 0.5 PFU/cell of HSV-GFP$^+$ virus and the numbers of GFP$^+$ cells were monitored by FACS. In addition, RS cells were grown to near confluence in Lab-Tex chamber slides and incubated with 50 μM 2-BP and then infected with VC1 virus for 24 h. UL20, gC, and gK were detected in live and fixed cells by confocal microscopy as described above.

Detection of UL20 palmitoylation. UL20 palmitoylation was determined using a modification of a procedure described previously (59). Briefly, RS cells were infected with VC1 virus (1 PFU/cell) in medium containing the specified concentration of 2-bromopalmitate (2-BP) (Sigma-Aldrich, St. Louis, MO), an inhibitor of palmitoylation. The 2-BP was dissolved in DMSO prior to addition to the medium. The concentration of DMSO in the medium did not exceed 1 μl/ml, and medium containing an equivalent volume of DMSO was used as a control. At 24 h postinfection, cells were washed with cold PBS and lysed in lysis buffer (LB) at pH 7.5 (50 mM Tris-HCl, 150 mM NaCl, 10% glycerol, 0.5% NP-40) with protease inhibitors (Roche, Indianapolis, IN), which was supplemented with 50 mM *N*-ethylmaleimide (NEM) (Sigma-Aldrich), which irreversibly blocks unmodified cysteine thiol groups. The cell lysates were cleared and then incubated with anti-FLAG antibody overnight at 4°C. Protein A/G beads were added to the lysate, incubated for another 2 h at 4°C, and washed with lysis buffer (LB) (pH 7.5) with protease inhibitors and 10 mM NEM and then with LB (pH 7.2) with protease inhibitors and 10 mM NEM. After resuspension in LB (pH 7.2), one-half was incubated with LB (pH 7.2) with protease inhibitors and 1 M hydroxylamine (HAM; Sigma-Aldrich), and one-half was incubated in the same buffer but without HAM as a control. After incubation for 1 h at room temperature, the beads were washed with LB (pH 6.2, with protease inhibitors) and incubated with LB (pH 6.2, with protease inhibitors) with 5 μM biotin-BMCC (Thermo Scientific, Asheville, NC) for 1 h at 4°C to label the exposed cysteines. After being washed with LB at pH 6.2 and at pH 7.5, the beads were incubated in 2× lithium dodecyl sulfate (LDS) buffer (Life Technologies, Carlsbad, CA) for 10 min at 80°C. The eluted samples were subjected to SDS-PAGE and then transferred to a polyvinylidene difluoride (PVDF) membrane. The palmitoylation signal was assessed using horseradish peroxidase (HRP)-conjugated streptavidin to detect the biotin label. The membrane was then stripped, and the levels of UL20 protein were assessed by Western blotting using anti-FLAG antibody and HRP-conjugated anti-mouse secondary antibody.

UL20 palmitoylation by GODZ. The construction of the C-terminally GFP-tagged GODZ dominant-negative mutant GFP-GODZ^{C157S} was described previously (12, 15) (Fig. 1D). HeLa cells were transfected with GFP-GODZ^{C157S} and UL20-V5 plasmids or GFP-Vector and UL20-V5 plasmids as controls. At 48 h posttransfection, GFP$^+$ cells were sorted by FACS, and 469,000 GFP$^+$ cells per treatment were lysed in lysis buffer as described above. The cell lysates were cleared and then incubated with anti-V5 antibody overnight at 4°C. Protein A/G beads were added to the lysate as described above. After resuspension in LB buffer, one-half was incubated with 1 M hydroxylamine (HAM; Sigma-Aldrich), and one-half was incubated in the same buffer but without HAM as a control. After incubation for 1 h at room temperature, the beads were washed, incubated with 5 μm biotin-BMCC (Thermo Scientific, Asheville, NC), washed again, and incubated in 2× LDS buffer (Life Technologies, Carlsbad, CA) for 10 min at 80°C as described above. The eluted samples were subjected to SDS-PAGE and then transferred to a PVDF membrane. The palmitoylation signal was assessed using HRP-conjugated streptavidin to detect the biotin label. The

level of UL20 protein for each treatment was assessed by Western blotting using anti-V5 antibody and HRP-conjugated anti-mouse secondary antibody.

Statistical analyses. Student's *t* test was performed using the computer program Instat (GraphPad, San Diego). Results were considered statistically significant when the *P* value was <0.05.

SUPPLEMENTAL MATERIAL

Supplemental material for this article may be found at https://doi.org/10.1128/JVI.00945-17.

SUPPLEMENTAL FILE 1, PDF file, 0.1 MB.

ACKNOWLEDGMENT

This work was supported by Public Health Service grant RO1 EY13615 to H.G.

REFERENCES

1. Klupp BG, Kern H, Mettenleiter TC. 1992. The virulence-determining genomic BamHI fragment 4 of pseudorabies virus contains genes corresponding to the UL15 (partial), UL18, UL19, UL20, and UL21 genes of herpes simplex virus and a putative origin of replication. Virology 191:900–908. https://doi.org/10.1016/0042-6822(92)90265-Q.
2. Davison AJ, Scott JE. 1986. The complete DNA sequence of varicella-zoster virus. J Gen Virol 67:1759–1816. https://doi.org/10.1099/0022-1317-67-9-1759.
3. Vlcek C, Benes V, Lu Z, Kutish GF, Paces V, Rock D, Letchworth GJ, Schwyzer M. 1995. Nucleotide sequence analysis of a 30-kb region of the bovine herpesvirus 1 genome which exhibits a colinear gene arrangement with the UL21 to UL4 genes of herpes simplex virus. Virology 210:100–108. https://doi.org/10.1006/viro.1995.1321.
4. Hatama S, Jang HK, Izumiya Y, Cai JS, Tsushima Y, Kato K, Miyazawa T, Kai C, Takahashi E, Mikami T. 1999. Identification and DNA sequence analysis of the Marek's disease virus serotype 2 genes homologous to the herpes simplex virus type 1 UL20 and UL21. J Vet Med Sci 61:587–593. https://doi.org/10.1292/jvms.61.587.
5. Agelidis AM, Shukla D. 2015. Cell entry mechanisms of HSV: what we have learned in recent years. Future Virol 10:1145–1154. https://doi.org/10.2217/fvl.15.85.
6. McGeoch DJ, Dalrymple MA, Davison AJ, Dolan A, Frame MC, McNab D, Perry LJ, Scott JE, Taylor P. 1988. The complete DNA sequence of the long unique region in the genome of herpes simplex virus type 1. J Gen Virol 69:1531–1574. https://doi.org/10.1099/0022-1317-69-7-1531.
7. Baines JD, Ward PL, Campadelli-Fiume G, Roizman B. 1991. The UL20 gene of herpes simplex virus 1 encodes a function necessary for viral egress. J Virol 65:6414–6424.
8. Foster TP, Melancon JM, Baines JD, Kousoulas KG. 2004. The herpes simplex virus type 1 UL20 protein modulates membrane fusion events during cytoplasmic virion morphogenesis and virus-induced cell fusion. J Virol 78:5347–5357. https://doi.org/10.1128/JVI.78.10.5347-5357.2004.
9. Fuchs W, Klupp BG, Granzow H, Mettenleiter TC. 1997. The UL20 gene product of pseudorabies virus functions in virus egress. J Virol 71:5639–5646.
10. Foster TP, Melancon JM, Olivier TL, Kousoulas KG. 2004. Herpes simplex virus type 1 glycoprotein K and the UL20 protein are interdependent for intracellular trafficking and trans-Golgi network localization. J Virol 78:13262–13277. https://doi.org/10.1128/JVI.78.23.13262-13277.2004.
11. Liu J, Lewin AS, Tuli SS, Ghivizzani SC, Schultz GS, Bloom DC. 2008. Reduction in severity of a herpes simplex virus type 1 murine infection by treatment with a ribozyme targeting the UL20 gene RNA. J Virol 82:7467–7474. https://doi.org/10.1128/JVI.02720-07.
12. Fang C, Deng L, Keller CA, Fukata M, Fukata Y, Chen G, Luscher B. 2006. GODZ-mediated palmitoylation of GABA(A) receptors is required for normal assembly and function of GABAergic inhibitory synapses. J Neurosci 26:12758–12768. https://doi.org/10.1523/JNEUROSCI.4214-06.2006.
13. Fukata M, Fukata Y, Adesnik H, Nicoll RA, Bredt DS. 2004. Identification of PSD-95 palmitoylating enzymes. Neuron 44:987–996. https://doi.org/10.1016/j.neuron.2004.12.005.
14. Sharma C, Rabinovitz I, Hemler ME. 2012. Palmitoylation by DHHC3 is critical for the function, expression, and stability of integrin alpha6beta4. Cell Mol Life Sci 69:2233–2244. https://doi.org/10.1007/s00018-012-0924-6.
15. Keller CA, Yuan X, Panzanelli P, Martin ML, Alldred M, Sassoe-Pognetto M, Luscher B. 2004. The gamma2 subunit of GABA(A) receptors is a substrate for palmitoylation by GODZ. J Neurosci 24:5881–5891. https://doi.org/10.1523/JNEUROSCI.1037-04.2004.
16. Mitchell DA, Vasudevan A, Linder ME, Deschenes RJ. 2006. Protein palmitoylation by a family of DHHC protein S-acyltransferases. J Lipid Res 47:1118–1127. https://doi.org/10.1194/jlr.R600007-JLR200.
17. Batistic O. 2012. Genomics and localization of the Arabidopsis DHHC-cysteine-rich domain S-acyltransferase protein family. Plant Physiol 160:1597–1612. https://doi.org/10.1104/pp.112.203968.
18. Greaves J, Chamberlain LH. 2011. DHHC palmitoyl transferases: substrate interactions and (patho)physiology. Trends Biochem Sci 36:245–253. https://doi.org/10.1016/j.tibs.2011.01.003.
19. Young FB, Butland SL, Sanders SS, Sutton LM, Hayden MR. 2012. Putting proteins in their place: palmitoylation in Huntington disease and other neuropsychiatric diseases. Prog Neurobiol 97:220–238. https://doi.org/10.1016/j.pneurobio.2011.11.002.
20. Du K, Murakami S, Sun Y, Kilpatrick C, Luscher B. 2017. DHHC7 palmitoylates Glut4 and regulates Glut4 membrane translocation. J Biol Chem 292:2979–2991. https://doi.org/10.1074/jbc.M116.747139.
21. Yeste-Velasco M, Linder ME, Lu YJ. 2015. Protein S-palmitoylation and cancer. Biochim Biophys Acta 1856:107–120. https://doi.org/10.1016/j.bbcan.2015.06.004.
22. Oh Y, Jeon YJ, Hong GS, Kim I, Woo HN, Jung YK. 2012. Regulation in the targeting of TRAIL receptor 1 to cell surface via GODZ for TRAIL sensitivity in tumor cells. Cell Death Differ 19:1196–1207. https://doi.org/10.1038/cdd.2011.209.
23. Uemura T, Mori H, Mishina M. 2002. Isolation and characterization of Golgi apparatus-specific GODZ with the DHHC zinc finger domain. Biochem Biophys Res Commun 296:492–496. https://doi.org/10.1016/S0006-291X(02)00900-2.
24. Kilpatrick CL, Murakami S, Feng M, Wu X, Lal R, Chen G, Du K, Luscher B. 2016. Dissociation of Golgi-associated DHHC-type zinc finger protein (GODZ)- and Sertoli cell gene with a zinc finger domain-beta (SERZ-beta)-mediated palmitoylation by loss of function analyses in knock-out mice. J Biol Chem 291:27371–27386. https://doi.org/10.1074/jbc.M116.732768.
25. Linder ME, Deschenes RJ. 2007. Palmitoylation: policing protein stability and traffic. Nat Rev Mol Cell Biol 8:74–84. https://doi.org/10.1038/nrm2084.
26. Fukata Y, Fukata M. 2010. Protein palmitoylation in neuronal development and synaptic plasticity. Nat Rev Neurosci 11:161–175. https://doi.org/10.1038/nrn2788.
27. El-Husseini AE, Craven SE, Chetkovich DM, Firestein BL, Schnell E, Aoki C, Bredt DS. 2000. Dual palmitoylation of PSD-95 mediates its vesiculotubular sorting, postsynaptic targeting, and ion channel clustering. J Cell Biol 148:159–172. https://doi.org/10.1083/jcb.148.1.159.
28. Allen SJ, Mott KR, Matsuura Y, Moriishi K, Kousoulas KG, Ghiasi H. 2014. Binding of HSV-1 glycoprotein K (gK) to signal peptide peptidase (SPP) is required for virus infectivity. PLoS One 9:e85360. https://doi.org/10.1371/journal.pone.0085360.
29. Altschul SF, Gish W, Miller W, Myers EW, Lipman DJ. 1990. Basic local alignment search tool. J Mol Biol 215:403–410. https://doi.org/10.1016/S0022-2836(05)80360-2.
30. Jambunathan N, Chowdhury S, Subramanian R, Chouljenko VN, Walker JD, Kousoulas KG. 2011. Site-specific proteolytic cleavage of the amino terminus of herpes simplex virus glycoprotein K on virion particles

inhibits virus entry. J Virol 85:12910–12918. https://doi.org/10.1128/JVI.06268-11.
31. Rathenberg J, Kittler JT, Moss SJ. 2004. Palmitoylation regulates the clustering and cell surface stability of GABAA receptors. Mol Cell Neurosci 26:251–257. https://doi.org/10.1016/j.mcn.2004.01.012.
32. Webb Y, Hermida-Matsumoto L, Resh MD. 2000. Inhibition of protein palmitoylation, raft localization, and T cell signaling by 2-bromopalmitate and polyunsaturated fatty acids. J Biol Chem 275:261–270. https://doi.org/10.1074/jbc.275.1.261.
33. Li X, Yang Y, Hu Y, Dang D, Regezi J, Schmidt BL, Atakilit A, Chen B, Ellis D, Ramos DM. 2003. Alphavbeta6-Fyn signaling promotes oral cancer progression. J Biol Chem 278:41646–41653. https://doi.org/10.1074/jbc.M306274200.
34. Chenette EJ, Abo A, Der CJ. 2005. Critical and distinct roles of amino- and carboxyl-terminal sequences in regulation of the biological activity of the Chp atypical Rho GTPase. J Biol Chem 280:13784–13792. https://doi.org/10.1074/jbc.M411300200.
35. Foster TP, Chouljenko VN, Kousoulas KG. 2008. Functional and physical interactions of the herpes simplex virus type 1 UL20 membrane protein with glycoprotein K. J Virol 82:6310–6323. https://doi.org/10.1128/JVI.00147-08.
36. Foster TP, Kousoulas KG. 1999. Genetic analysis of the role of herpes simplex virus type 1 glycoprotein K in infectious virus production and egress. J Virol 73:8457–8468.
37. Hutchinson L, Johnson DC. 1995. Herpes simplex virus glycoprotein K promotes egress of virus particles. J Virol 69:5401–5413.
38. Hutchinson L, Roop-Beauchamp C, Johnson DC. 1995. Herpes simplex virus glycoprotein K is known to influence fusion of infected cells, yet is not on the cell surface. J Virol 69:4556–4563.
39. David AT, Baghian A, Foster TP, Chouljenko VN, Kousoulas KG. 2008. The herpes simplex virus type 1 (HSV-1) glycoprotein K (gK) is essential for viral corneal spread and neuroinvasiveness. Curr Eye Res 33:455–467. https://doi.org/10.1080/02713680802130362.
40. Jayachandra S, Baghian A, Kousoulas KG. 1997. Herpes simplex virus type 1 glycoprotein K is not essential for infectious virus production in actively replicating cells but is required for efficient envelopment and translocation of infectious virions from the cytoplasm to the extracellular space. J Virol 71:5012–5024.
41. Allen SJ, Mott KR, Ghiasi H. 2014. Inhibitors of signal peptide peptidase (SPP) affect HSV-1 infectivity in vitro and in vivo. Exp Eye Res 123:8–15. https://doi.org/10.1016/j.exer.2014.04.004.
42. Lemberg MK, Martoglio B. 2002. Requirements for signal peptide peptidase-catalyzed intramembrane proteolysis. Mol Cell 10:735–744. https://doi.org/10.1016/S1097-2765(02)00655-X.
43. Beel AJ, Sanders CR. 2008. Substrate specificity of gamma-secretase and other intramembrane proteases. Cell Mol Life Sci 65:1311–1334. https://doi.org/10.1007/s00018-008-7462-2.
44. Greaves J, Chamberlain LH. 2007. Palmitoylation-dependent protein sorting. J Cell Biol 176:249–254. https://doi.org/10.1083/jcb.200610151.
45. Buglino JA, Resh MD. 2008. Hhat is a palmitoylacyltransferase with specificity for N-palmitoylation of Sonic Hedgehog. J Biol Chem 283:22076–22088. https://doi.org/10.1074/jbc.M803901200.
46. Draper JM, Smith CD. 2009. Palmitoyl acyltransferase assays and inhibitors (review). Mol Membr Biol 26:5–13. https://doi.org/10.1080/09687680802683839.
47. Conibear E, Davis NG. 2010. Palmitoylation and depalmitoylation dynamics at a glance. J Cell Sci 123:4007–4010. https://doi.org/10.1242/jcs.059287.
48. Nozawa N, Daikoku T, Koshizuka T, Yamauchi Y, Yoshikawa T, Nishiyama Y. 2003. Subcellular localization of herpes simplex virus type 1 UL51 protein and role of palmitoylation in Golgi apparatus targeting. J Virol 77:3204–3216. https://doi.org/10.1128/JVI.77.5.3204-3216.2003.
49. Baird NL, Starkey JL, Hughes DJ, Wills JW. 2010. Myristylation and palmitylation of HSV-1 UL11 are not essential for its function. Virology 397:80–88. https://doi.org/10.1016/j.virol.2009.10.046.
50. Ghiasi H, Bahri S, Nesburn AB, Wechsler SL. 1995. Protection against herpes simplex virus-induced eye disease after vaccination with seven individually expressed herpes simplex virus 1 glycoproteins. Invest Ophthalmol Vis Sci 36:1352–1360.
51. Ghiasi H, Kaiwar R, Nesburn AB, Slanina S, Wechsler SL. 1994. Expression of seven herpes simplex virus type 1 glycoproteins (gB, gC, gD, gE, gG, gH, and gI): comparative protection against lethal challenge in mice. J Virol 68:2118–2126.
52. Ghiasi H, Cai S, Slanina S, Nesburn AB, Wechsler SL. 1997. Nonneutralizing antibody against the glycoprotein K of herpes simplex virus type-1 exacerbates herpes simplex virus type-1-induced corneal scarring in various virus-mouse strain combinations. Invest Ophthalmol Vis Sci 38:1213–1221.
53. Allen SJ, Mott KR, Ljubimov AV, Ghiasi H. 2010. Exacerbation of corneal scarring in HSV-1 gK-immunized mice correlates with elevation of $CD8^+$ $CD25^+$ T cells in corneas of ocularly infected mice. Virology 399:11–22. https://doi.org/10.1016/j.virol.2009.12.011.
54. Perng GC, Dunkel EC, Geary PA, Slanina SM, Ghiasi H, Kaiwar R, Nesburn AB, Wechsler SL. 1994. The latency-associated transcript gene of herpes simplex virus type 1 (HSV-1) is required for efficient in vivo spontaneous reactivation of HSV-1 from latency. J Virol 68:8045–8055.
55. Ghiasi H, Slanina S, Nesburn AB, Wechsler SL. 1994. Characterization of baculovirus-expressed herpes simplex virus type 1 glycoprotein K. J Virol 68:2347–2354.
56. Allen SJ, Mott KR, Ghiasi H. 2014. Overexpression of herpes simplex virus glycoprotein K (gK) alters expression of HSV receptors in ocularly-infected mice. Invest Ophthalmol Vis Sci 55:2442–2451. https://doi.org/10.1167/iovs.14-14013.
57. Elliott G, O'Hare P. 1999. Intercellular trafficking of VP22-GFP fusion proteins. Gene Ther 6:149–151. https://doi.org/10.1038/sj.gt.3300850.
58. Elliott G, O'Hare P. 1999. Live-cell analysis of a green fluorescent protein-tagged herpes simplex virus infection. J Virol 73:4110–4119.
59. Brigidi GS, Bamji SX. 2013. Detection of protein palmitoylation in cultured hippocampal neurons by immunoprecipitation and acyl-biotin exchange (ABE). J Vis Exp 72:50031. https://doi.org/10.3791/50031.